

# Etching and forward transfer of fused silica in solid-phase by femtosecond laser-induced solid etching (LISE)

David P. Banks<sup>\*,a,1</sup>, Kamal S. Kaur<sup>a</sup>, Robert W. Eason<sup>a</sup>

<sup>a</sup>*Optoelectronics Research Centre, University of Southampton, Southampton UK SO17 1BJ*

---

## Abstract

We present a femtosecond laser-based technique for etching and forward transfer of bulk transparent materials in solid phase. Femtosecond laser pulses with  $\lambda = 800$  nm were focused through a fused silica block onto an absorbing thin film of Cr. A constraining Si wafer was pressed into tight contact with the Cr film to prevent lift-off of the film. A combination of the high temperature and pressure of the Cr, and compressive stress from the Si, resulted in etching of smooth features from the fused silica by cracking. Unlike in conventional ablative or chemical etching, the silica was removed from the bulk as single solid-phase pieces which could be collected on the Si. Using this so-called laser-induced solid etching (LISE) technique, 1-2  $\mu\text{m}$  deep pits and channels have been produced in the silica surface, and corresponding dots and lines deposited on the Si. The threshold fluence for etching was

---

\*Corresponding author

*Email address:* [dpb@orc.soton.ac.uk](mailto:dpb@orc.soton.ac.uk) (David P. Banks)

<sup>1</sup>Tel.: +44 2380593144

found to be  $\approx 0.4 \text{ J/cm}^2$  with  $\approx 130 \text{ fs}$  duration pulses. The morphology of the etched features are investigated as functions of fluence and exposure to multiple pulses.

*Key words:* femtosecond, forward transfer, etching, fracture, deposition

*PACS:* xx.xx-x

---

## 1. Introduction

Laser-induced forward transfer (LIFT) techniques offer a simple and versatile method for the micro-deposition of a range of materials [1, 2, 3, 4, 5, 6]. Although metals [1, 7, 8], polymers [9, 10], oxides [11], semiconductors [12], superconductors [13], diamond [14], carbon nanotubes [15], and biomaterials [16, 17] have now been successfully deposited using LIFT, the forward transfer of solid transparent materials is still challenging.

In LIFT, focused or demagnified laser pulses are used to drive pixelated transfer of a single- or multi-component source film (the *donor*) coated onto the backside of a transparent (*carrier*) substrate. The forward transferred donor material is then collected on another substrate placed nearby (typically  $\leq 5 \mu\text{m}$  away: the *receiver*) (see fig. 1). Typically LIFT techniques rely on direct absorption of the laser light used in the printing process in the donor material, which necessarily leads to transfer of film material by melting or ablation [7]. In a recent work, we demonstrated the transfer of Cr in solid, single-pieces by using multiple low energy pulses to gently delaminate and release the donor material [8].

Multi-photon absorption of femtosecond duration pulses has recently allowed for the LIFT of transparent donors. Zergioti et al. and Mailis et al. have demonstrated transfer of transparent ITO films [18, 19], and recently we reported the transfer of a transparent gadolinium gallium oxide (GdGaO) film [20]. However, the resultant deposits in all these cases exhibited significant surface roughness and appeared to have been transferred as molten fragments. Much smoother and unshattered deposits of GdGaO were obtained using a sacrificial dynamic release layer (DRL [2]) of nitrogen-releasing triazene polymer (TP [21]) to provide the thrust for LIFT [20]. However, the TP dissociates at around 250°C [21] and is sensitive to solvent treatment, thereby limiting the choice of donor materials that can be deposited on top. Using more robust materials such as metals for the DRL (see e.g. [16]) can result in residual, undecomposed DRL being mixed with, or remaining on top of, the transferred donor [22].

In this work, we present a new LIFT technique (which we call laser-induced solid etching (LISE)) that allows transparent material to be transferred in solid-phase contiguous pieces. By utilising controlled laser cracking rather than direct ablation, LISE allows for the forward transfer of transparent materials with surface smoothness comparable to the best achievable with DRL-LIFT [20]. The key difference from conventional LIFT is that the material transferred is etched from the transparent carrier substrate instead of the donor film. Using LISE, the forward transfer deposition of fused silica has been achieved for the first time. Furthermore, as the transferred material

is etched from the bulk carrier, the features deposited on the receiver correspond exactly to structures etched into the backside of the carrier. Hence, LISE can also be used as a method of direct-writing onto the backside of UV-transparent substrates. Again, the LISE method compares well in terms of processing speed, simplicity, and feature quality with existing backside writing techniques [23, 24].

### *1.1. Backside writing*

To process UV-transparent materials with nanosecond or longer pulsed lasers, it is possible to use either extremely high powers [25], or to include a laser absorbing material. This absorber can be in the form of a dopant, but in many real applications doping of the target material is undesirable, or as a thin film coating that must be removed after patterning.

An alternative approach that has been extensively investigated is backside etching. This approach utilises laser absorption in an absorbing material in contact with the UV-transparent substrate. The processing laser is focused through the substrate onto the absorber-substrate interface where rapid boiling of the absorber etches away some of the substrate. This technique is known as laser-induced backside wet etching (LIBWE [23, 26]) or dry etching (LIBDE [24, 27]) depending on whether the absorber is a solution or solid (often metallic) film. With LIBWE, etch rates of 10s nm/pulse are typically reported [23, 26] and the resultant features can be very smooth and uniform. However, the process requires a specialised liquid chamber,

potentially harmful solvents, and can be complicated to carry out in practice. LIBDE has been shown to be capable of a much higher etch rate ( $\approx 500$  nm/pulse for a single pulse [24] up to  $\approx 1 \mu\text{m}$  with 3-5 pulses [28]) and is much simpler, but the etched features are typically somewhat rougher than with LIBWE. Both these backside etching techniques eliminate the problem of redeposited debris inherent with ablative microstructuring.

### *1.2. Laser-induced cracking*

The formation and growth of cracks in, particularly, fused silica has been studied extensively in recent years because of the impact on the lifetime of high power and remote (e.g. satellite-based) optical systems [29, 30, 31]. It has been observed that exposure to multiple laser pulses leads to a crack originating on the backside of transparent substrates, which grows backwards into the substrate along the laser propagation axis. Dahmani et al. [30, 31] have observed a dependence of the crack morphology on stress applied parallel to the laser propagation axis. When no external stress was applied, cracks with a diameter of approximately the laser spot size at the substrate surface penetrating mm into the silica were seen. However, if the applied stress was increased to  $\approx 41$  kPa, the silica damage was manifested as a smooth-sided 100-200  $\mu\text{m}$  deep pit, again with a diameter approximately the same as the spot size [30]. This stress-suppressed cracking forms the basis of the LISE process.

### 1.3. Laser-induced solid etching (LISE)

The LISE process combines elements of LIFT, LIBDE, and laser cracking for the solid-phase etching and forward transfer of brittle, transparent bulk substrates (fig. 2). An absorbing thin film (referred to as a *shock-generation layer* (SGL)) is coated onto the backside of a transparent substrate, as in LIFT or LIBDE, and a second bulk substrate, akin to the receiver in a LIFT setup, is pressed into tight contact with the thin film. Femtosecond laser pulses are then focused or demagnified through the transparent substrate onto the film, where they are absorbed, leading to very large and rapid pressure and temperature increases in the film (fig. 2(a)). The film can reach pressures up to 10s-100s GPa [32, 33, 34, 35], and temperatures of up to 1000s K [36, 37].

The extremely high temperature and pressure in the SGL can cause secondary damage to the surface of the transparent substrate, as in LIBDE [24] (fig. 2(b)). This damage, which is localised to the irradiated area, then acts as the seed for crack propagation into the bulk of the substrate [29, 31]. However, because of the tight contact between the substrates and the SGL, there is a compressive stress on the bulk substrates. Hence, crack propagation into the bulk is impeded, and instead the etched features appear as smooth pits on the surface after exposure to multiple pulses, like those reported by Dahmani et al. [30] (fig. 2(c,d)).

## 2. Experimental

To study the LISE process, 50 mm diameter, 6 mm thick discs of fused silica were coated with  $\approx 80$  nm of Cr by thermal evaporation. The coated face of a silica disc was pressed into tight contact with a Si wafer in a vacuum cell held at a pressure of  $\approx 10$  Pa. Note that the silica acted as the top window of the vacuum cell. Hence, the pressure difference across the silica window was around  $10^5$  Pa and so when the Si wafer was brought into tight contact, the compressive stresses on the silica was similar to the 10s kPa applied to get relatively smooth silica pits by Dahmani et al. [30].

Femtosecond duration pulses (800 nm, 110 fs) with a Gaussian spatial profile ( $1/e^2$  diameter of  $\approx 4$  mm) from a Ti:sapphire laser (Coherent MIRA and Legend) illuminated an  $\approx 450$   $\mu\text{m}$  circular aperture at a repetition rate of 250 Hz. An image of the aperture was then relayed to the silica-Cr interface by a reverse-projection microscope to give an  $\approx 10$   $\mu\text{m}$  diameter, roughly uniform intensity circular spot. The vacuum cell was mounted on a 3-axis, computer-controlled translation stage and high-speed mechanical shutter (Uniblitz LS3) was used to control laser exposure.

## 3. Results and discussion

### 3.1. LISE of fused silica domes

The first experiments concerned the transfer of single,  $\approx 10$   $\mu\text{m}$  spots of silica onto the Si substrate by LISE. It was observed that two thresholds

existed for the LISE process; a threshold fluence below which no transfer occurred, and a minimum number of pulses that were required to etch the silica. The threshold fluence was measured to be  $0.37 \text{ J/cm}^2$ , which approximately coincided with the onset of ablation in the SGL [7].

Figure 3 shows a sequence of SEM micrographs of silica deposits on the Si surface after exposure to an increasing number of pulses,  $N_p$ , at a fluence of  $0.4 \text{ J/cm}^2$ , i.e. just above the transfer threshold. It can be seen that the first few pulses (up to around  $N_p = 20$ ) simply repeatedly melted and ablated the SGL, leaving some remaining on the Si and some on the silica (not shown here). The threshold for silica etching in this case appeared around  $N_p = 20 - 30$ .

For  $N_p \geq 30$ , domed deposits of fused silica that had been etched from the bulk substrate were consistently seen on the Si surface. Similar deposits were obtained over a very broad range of  $N_p$ , up to 1000-2000. Observation of the deposits obtained with  $N_p \geq 2000$  revealed that exposure to very high numbers of pulses resulted in damage to the underlying Si. This finding suggested that, when using LISE for forward transfer, it is important to use only sufficient pulses to transfer the transparent material as any subsequent pulses can pass through the deposited material and damage the underlying substrate.

An interesting point to note is that the machined features in the silicon obtained with large  $N_p$  appeared to be much smoother than those usually seen with direct ablation. As such it is believed that these structures were



the result of LISE of the Si substrate. It appears therefore, that LISE may be suitable for the etching of smooth structures in the surface of absorbing substrates as well.

It would be tempting to conclude that the dome-shaped features were the result of redeposition of particulate material gradually etched out of the transparent substrate by boiling of the SGL (as in LIBDE). However, closer inspection revealed that many of the silica deposits exhibited sharp features and edges that could only have been the result of the deposit being etched from the transparent substrate and transferred as a single, solid piece (see, e.g.  $N_p = 100, 200, 300, 500, 2000$  fig. 3). These features could also be seen in the corresponding holes in the silica substrate, confirming that the deposits must have been transferred as a single piece. Figure 4(a) shows an SEM micrograph of a silica hole and fig. 4(b) shows a micrograph of the corresponding deposit on the Si after exposure to 500 pulses with fluence  $0.4 \text{ J/cm}^2$ . A couple of features can be seen in fig. 4 that conclusively prove etching as a single, solid-phase piece; firstly, the edges of the hole and deposit corresponded exactly (e.g. the boxed regions marked 'A' in the figure), and second, sharp discontinuities could be seen in both the hole and the deposit (e.g. regions 'B').

Obtaining good adherence of material deposited by forward transfer techniques is a challenge. With the current LISE setup, the repeatedly melted and resolidified Cr SGL between the silica and Si substrates provided an excellent bonding layer. The silica deposits were observed to remain on the Si

surface after 5 minutes in an ultrasound bath in deionised water at 40°C.

### 3.2. LISE of silica lines

The second half of our initial study of the LISE of fused silica concentrated on the direct-writing of continuous lines. These structures were obtained using an identical setup as described above except that the laser was raster scanned across the sample with speed  $v$  mm/s (recall that the laser repetition rate was 250 Hz and the spot diameter at the silica-SGL interface was  $\approx 10$   $\mu\text{m}$ ).

Figure 5 shows SEM micrographs of the resultant structures seen on the Si surface after exposure to fluences from 0.3 J/cm<sup>2</sup> (fig. 5(a)) to 1 J/cm<sup>2</sup> (fig. 5(h)) with a raster speed of  $v = 1.1$  mm/s. As was the case with the dome-shaped structures in the previous section, a well-defined fluence threshold was observed; in this case the threshold was between 0.5 and 0.6 J/cm<sup>2</sup>. Below this fluence threshold, only the SGL was transferred to the Si, resulting in relatively uniform Cr lines. Once the LISE threshold fluence was reached, continuous silica lines 1-2  $\mu\text{m}$  in height were deposited. It was observed that the smoothness of the lines improved with increasing fluence. This was in agreement with the cracking results of Dahmani et al., where it was observed that increasing the compressive stress on the transparent substrate resulted in smoother pits [30].

The higher fluence threshold for LISE measured with the lines than with the silica domes can be partially explained by the fact that, due to rastering of

the laser, there was less overlapping of multiple pulses when writing the lines. However, with the dome-shaped deposits, it was observed that a minimum of 10-20 pulses were required to LISE the silica. The lines shown in fig. 5 were written with  $v = 1.1$  mm/s, which with a spot size of  $\approx 10$   $\mu\text{m}$  and repetition rate of 250 Hz, corresponded approximately to a  $\approx 55 - 60\%$  overlap between successive pulses. Therefore, we must conclude that the lines were the result of a cumulative cracking process that was initiated at the point where the translation stage was accelerating, and hence where there was more overlapping of multiple pulses. The channel formed by the cracking then propagated along the silica surface, becoming incrementally longer with each successive pulse, as the laser was scanned across the target.

Clearly the silica deposition process corresponded to etching of the transparent substrate and so there were channels left in the silica surface after LISE. A detailed study of the channels as a function of processing parameters will be reported separately; here we just present a visual examination of the channels. Figure 6 shows SEM micrographs of the Cr-coated silica surface after LISE (the Cr was left on to prevent surface charging in the SEM). With fluence below the LISE threshold ( $0.3$  J/cm<sup>2</sup>: fig. 6(a)), the Cr was not completely removed in the irradiated area and the silica was not etched. When the fluence was increased to greater than the previously identified LISE threshold to  $1$  J/cm<sup>2</sup>, and the raster speed was slow ( $\leq 0.9$  mm/s: fig. 6(b)), the Cr was completely removed from the silica surface, but again no channel was observed. Instead channel formation was only observed when the raster

speed was increased above a well-defined threshold; in this case  $\approx 0.9$  mm/s (fig. 6(c)). Closer examination of the channels (fig. 6(d)) revealed them to be smooth-sided, V-shaped features with only minimal evidence of redeposited material in the channel. The sharpness of the features again supported the hypothesis of etching by solid-phase cracking rather than ablation or boiling of the Cr.

Clearly, as with the silica domes, there were two thresholds for the LISE of the silica lines; a fluence threshold (which was higher for the lines than the domes because of fewer overlapping pulses) and a raster speed threshold (related to the overlapping of successive pulses). To understand how these two thresholds were related, the maximum heights of the lines on the Si were measured by stylus profiling as functions of fluence and raster speed. The results are shown in fig. 7. The Cr-only lines (i.e. no LISE of the silica) were around 100-250 nm thick, slightly thicker than the original SGL but this discrepancy can be explained by considering that the deposited Cr was much rougher than the original SGL film. The silica lines, on the other hand, were around 1-2  $\mu\text{m}$  in height, corresponding well with the height of the silica domes reported in section 3.1.

From fig. 7, it can be seen that, at the lowest raster speed (0.3 mm/s), no silica lines were deposited, independent of fluence. As the raster speed was increased, the threshold fluence for LISE of the silica was observed to decrease. Figure 8(a-h) shows SEM micrographs of the lines deposited with a fluence of  $0.7 \text{ J/cm}^2$  whilst varying  $v$ ; at this fluence, the threshold for

LISE of continuous silica lines was around  $v = 0.9$  mm/s. Observation of the lines obtained with  $v$  less than the raster speed threshold (fig. 8(a-c)) indicate why a raster speed threshold existed. The line produced with  $v = 0.1$  mm/s (fig. 8(a)) in particular exhibited an obviously damaged central region and edges where the deposited material appeared to be LISE deposited silica. At this speed, approximately 10 incident pulses overlapped at any given point. Hence, we conclude that the observed line was the result of a LISE-deposited silica line that was subsequently destroyed and partially redeposited in the original channel by exposure to too many high energy pulses. When the raster speed was increased to  $v = 0.9$  mm/s (fig. 8(d)), only 2 successive pulses overlapped at any given point. As a result, the LISE-deposited silica line was not destroyed by exposure to pulses incident after etching had occurred. Hence we can conclude that the LISE line-writing process has a fluence threshold that determines if LISE occurs, and a raster speed threshold to prevent post-etching damage of the transferred material.

Observing the lines obtained as  $v$  was increased further (fig. 8(e-h)) revealed a periodic variation of the lines with a period that matched the spacing between successive pulses. For example, with  $v = 1.5$  mm/s (fig. 8(g)) the pulse-to-pulse separation was around  $6 \mu\text{m}$ , closely matching the periodicity seen in the line structure. It was observed previously that LISE was not possible with single pulses. Hence, it is believed that the lines were the result of successive pulses propagating cracks in the silica along the line length. Once the raster speed became sufficiently great that the pulse-to-pulse spacing was

large compared to the spot size, continuous silica lines were not observed (the maximum speed was found to be  $v \approx 2$  mm/s at all studied fluences).

As a final point to note, with the correct exposure conditions, the uniformity of the silica lines was observed to be very good, with minimal variation observed over the full 0.5 mm writing length. As an example, fig. 8(i) shows an SEM micrograph of lines obtained with fluence  $1 \text{ J/cm}^2$  with  $v = 0.9$  (left), 1.1, 1.3, 1.5, and 1.7 (right) mm/s. The SEM micrograph in fig. 8(i) also clearly shows the variation in line morphology with increasing  $v$ . Lines written at slower speeds appeared to have smoother tops and straighter edges, whilst faster speeds resulted in increasingly segmented structures. At the highest speed in fig. 8(i) ( $v = 1.7$  mm/s), the contribution of each successive pulse adding a small section to the end of the line is clearly visible.

#### 4. Conclusions

We have presented initial studies of the LISE of fused silica. The high pressures and temperatures generated in a thin Cr film under femtosecond laser pulse irradiation combined with the compressive stress from tight contact with a Si wafer under vacuum resulted in etching of very smooth features in the silica. It was found that the threshold fluence required for etching ( $\approx 0.4 \text{ J/cm}^2$ ) approximately corresponded to the onset of ablation of the Cr. The etched silica was deposited onto the Si, allowing for the use of LISE as a solid-phase forward transfer technique. Adherence of the transferred material was found to be very good due to the presence of resolidified Cr

SGL between the Si substrate and deposited silica.

Using LISE, circular dome-like structures and continuous lines have been forward transferred (and corresponding pits and channels etched in the bulk fused silica). With the domes, the fluence threshold was *approx*  $0.4 \text{ J/cm}^2$  and around 20-30 pulses were necessary to achieve etching. With the line structures, the fluence threshold increased due to less spatial overlap between successive pulses, and a complicated interplay between laser fluence and writing speed was found. The best results in terms of line smoothness and uniformity were obtained with higher fluence ( $0.9\text{-}1 \text{ J/cm}^2$ ) and writing speeds that corresponded to a spatial overlap of successive pulses around 55-60%.

We also found some evidence of LISE of the underlying Si substrate when very many pulses were used. Smooth-sided pits were seen in the Si surface with a depth of  $\approx 3\text{-}4 \mu\text{m}$  when several 1000 pulses were incident. This process has not been investigated in detail, but suggests that LISE may also be a promising technique for the etching of smooth features in the surface of absorbing substrates.

## References

- [1] J. Bohandy, B. Kim, F. Adrian, J. Appl. Phys. 60 (1) (1986) 1538–1539.
- [2] W. Tolbert, I. Lee, M. Doxtader, E. Ellis, D. Dlott, J. Imag. Sci. Tech. 37 (4) (1993) 411–421.

- [3] H. Fukumura, Y. Kohji, K. Nagasawa, H. Masuhara, *J. Am. Chem. Soc.* 116 (1994) 10304–10305.
- [4] A. Pique, D. Chrisey, R. Auyeung, J. Fitz-Gerald, H. Wu, R. McGill, S. Lakeou, P. Wu, V. Nguyen, M. Duignan, *Appl. Phys. A [Suppl.]* 69 (1999) S279–S284.
- [5] D. Toet, M. Thompson, P. Smith, T. Sigmon, *Appl. Phys. Lett.* 74 (15) (1999) 2170–2172.
- [6] G. Blanchet, Y.-L. Loo, J. Rogers, F. Gao, C. Fincher, *Appl. Phys. Lett.* 82 (3) (2003) 463–465.
- [7] D. Banks, C. Grivas, J. Mills, I. Zergioti, R. Eason, *Appl. Phys. Lett.* 89 (2006) 193107.
- [8] D. Banks, C. Grivas, I. Zergioti, R. Eason, *Opt. Express* 16 (2008) 3249–3254.
- [9] J. Lee, S. Lee, *Adv. Mater.* 16 (1) (2004) 51–54.
- [10] B. Thomas, A. Alloncle, P. Delaporte, M. Sentis, S. Sanaur, M. Barret, P. Collot, *Appl. Surf. Sci.* 254 (2007) 1206–1210.
- [11] I. Zergioti, S. Mailis, N. Vainos, P. Papakonstantinou, C. Kalpouzos, C. Grigoropoulos, C. Fotakis, *Appl. Phys. A* 66 (1998) 579–582.
- [12] P. Mogyorosi, T. Szorenyi, K. Ball, Z. Toth, I. Hevesi, *Appl. Surf. Sci.* 36 (1989) 157–163.



- [13] E. Fogarassy, C. Fuchs, F. Kerherve, G. Hauchecorne, J. Perriere, J. Appl. Phys. 66 (1) (1989) 457–459.
- [14] S. Pimenov, G. Shafeev, A. Smolin, V. Konov, B. Vodolaga, Appl. Surf. Sci. 86 (1995) 208–212.
- [15] S. Chang-Jian, J. Ho, J. Cheng, C. Sung, Nanotechnology 17 (2006) 1184–1187.
- [16] P. Serra, M. Colina, J. Fernandez-Pradas, L. Sevilla, J. Morenza, Appl. Phys. A 85 (9) (2004) 1639–1641.
- [17] Y. Tsuboi, Y. Furuhata, N. Kitamura, Appl. Surf. Sci. 253 (2007) 8422–8427.
- [18] S. Mailis, I. Zergioti, G. Koundourakis, A. Ikiades, A. Patentalaki, P. Papanconstantinou, N. Vainos, C. Fotakis, Appl. Opt. 38 (11) (1999) 2301–2308.
- [19] I. Zergioti, D. Papazoglou, A. Karaiskou, N. Vainos, C. Fotakis, Appl. Surf. Sci. 197-198 (2002) 868–872.
- [20] D. Banks, K. Kaur, R. Gazia, R. Fardel, M. Nagel, T. Lippert, R. Eason, Europhys. Lett. 83 (2008) 38003.
- [21] M. Nagel, R. Hany, T. Lippert, M. Molberg, F. Nuesch, D. Rentsch, Macromol. Chem. Phys. 208 (2007) 277–286.

- [22] T. Smausz, B. Hopp, G. Kecskemeti, Z. Bor, *Appl. Surf. Sci.* 252 (2006) 4738–4742.
- [23] J. Wang, H. Niino, A. Yabe, *Appl. Phys. A* 68 (1) (1999) 111–113.
- [24] B. Hopp, C. Vass, T. Smausz, Z. Bor, *J. Phys. D: Appl. Phys.* 39 (2006) 48434847.
- [25] J. Ihlemann, B. Wolff-Rottke, *Appl. Surf. Sci.* 106 (1996) 282–286.
- [26] J. Wang, H. Niino, A. Yabe, *Appl. Surf. Sci.* 87 (2000) 45–53.
- [27] B. Hopp, C. Vass, T. Smausz, *Appl. Surf. Sci.* 253 (2007) 79227925.
- [28] T. Smausz, T. Csizmadia, N. Kresz, C. Vass, Z. Marton, B. Hopp, *Appl. Surf. Sci.* 254 (2007) 10911095.
- [29] A. Salleo, R. Chinsio, F. Genin, *Proc. SPIE* 3578 (1998) 456–471.
- [30] F. Dahmani, S. Burns, J. L. S. Papernov, A. Schmid, *Opt. Lett.* 24 (8) (1999) 516–518.
- [31] F. Dahmani, J. Lambropoulos, A. Schmid, S. Papernov, S. Burns, *Appl. Optics* 38 (33) (1999) 6892–6903.
- [32] T. Sano, H. Mori, O. Sakata, E. Ohmura, I. Miyamoto, A. Hirose, K. Kobayashi, *Appl. Surf. Sci.* 247 (2005) 571576.

- [33] R. Evans, A. Badger, F. Fallis, M. Mahdih, T. Hall, P. Audebert, J.-P. Geindre, J.-C. Gauthier, A. Mysyrowicz, G. Grillon, A. Antonetti, Phys. Rev. Lett. 77 (16) (1996) 3359–3362.
- [34] D. Moore, K. Gahagan, J. Reho, D. Funk, S. Buelow, R. Rabie, T. Lipfert, Appl. Phys. Lett. 78 (1) (2001) 40–42.
- [35] D. Funk, D. Moore, S. McGrane, K. Gahagan, J. Reho, S. Buelow, J. Nicholson, G. Fisher, R. Rabie, Thin Solid Films 453-454 (2004) 542549.
- [36] J. Hohlfeld, S.-S. Wellershoff, J. Gudde, U. Conrad, V. Jahnke, E. Matthias, Chem. Phys. 251 (2000) 237–258.
- [37] E. Gamaly, A. Rode, B. Luther-Davies, V. Tikhonchuk, Phys. Plasmas 9 (3) (2002) 949–957.
- [38] R. Stoian, A. Mermillod-Blondin, S. Winkler, A. Rosenfeld, I. Hertel, M. Spyridaki, E. Koudoumas, P. Tzanetakis, C. Fotakis, I. Burakov, N. Bulgakova, Opt. Eng. 45 (5) (2005) 051106.

Fig. 1 Schematic of the LIFT technique.

Fig. 2 Schematic of the LISE technique.

Fig. 3 SEM micrographs of deposits of fused silica produced by varying  $N_p$ , with fluence  $0.4 \text{ J/cm}^2$ .

Fig. 4 SEM micrographs of a hole in fused silica (a) and corresponding silica deposit on Si (b).  $N_p = 500$ , fluence  $0.4 \text{ J/cm}^2$ .

Fig. 5 SEM micrographs of line structures obtained by raster-scanning laser at  $v = 1.1 \text{ mm/s}$  with indicated fluence.

Fig. 6 SEM micrographs of channels in fused silica substrate after exposure to  $0.3 \text{ J/cm}^2$  (a) and  $1 \text{ J/cm}^2$  (b,c) with indicated raster speeds. Close up of channel with  $1 \text{ J/cm}^2$  written at  $1.1 \text{ mm/s}$  (d).

Fig. 7 Plot of maximum height of silica lines as a function of fluence and raster speed.

Fig. 8 SEM micrographs of line structures obtained by varying raster speed  $v$  with fluence  $0.7 \text{ J/cm}^2$  (a-h) and zoomed-out view of silica lines with  $1 \text{ J/cm}^2$  (i).

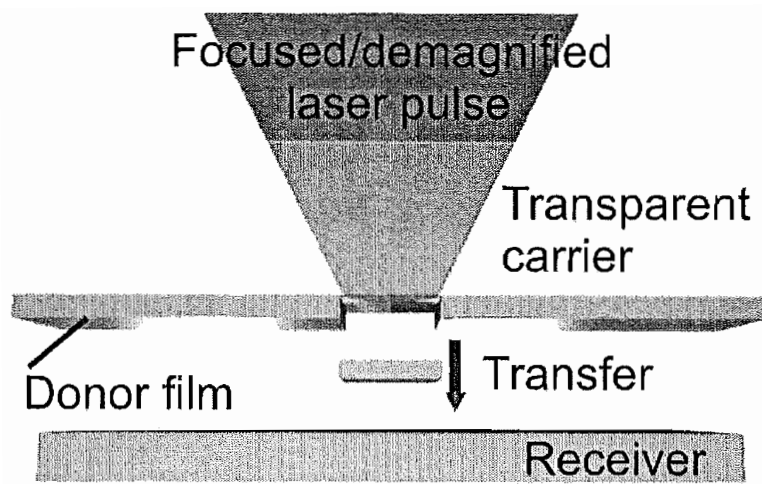


Figure 1: Schematic of the LIFT technique.

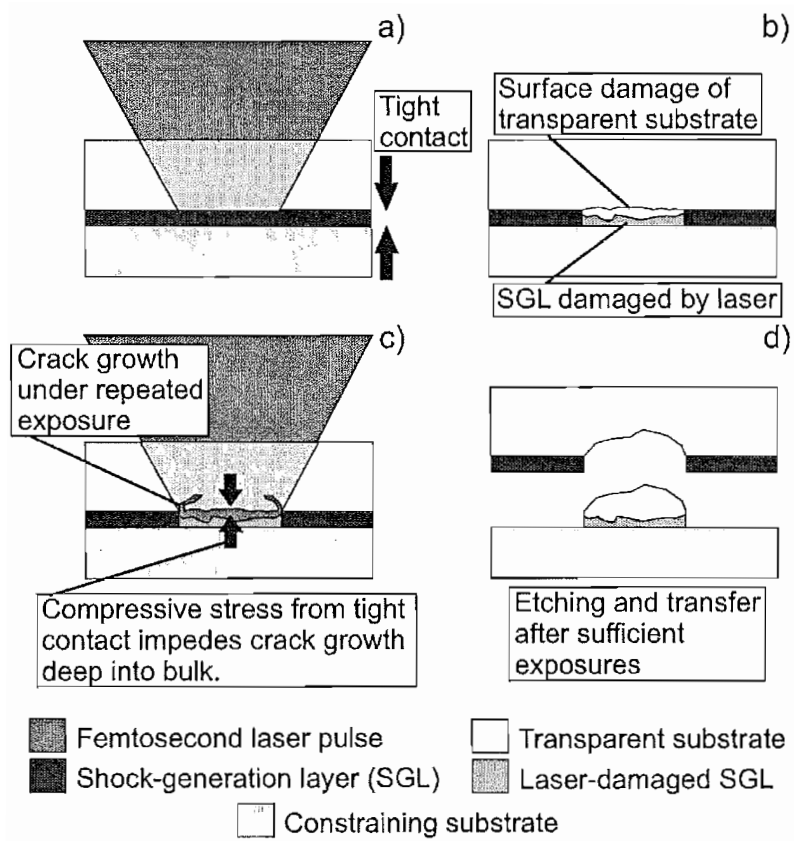


Figure 2: Schematic of the LISE technique.

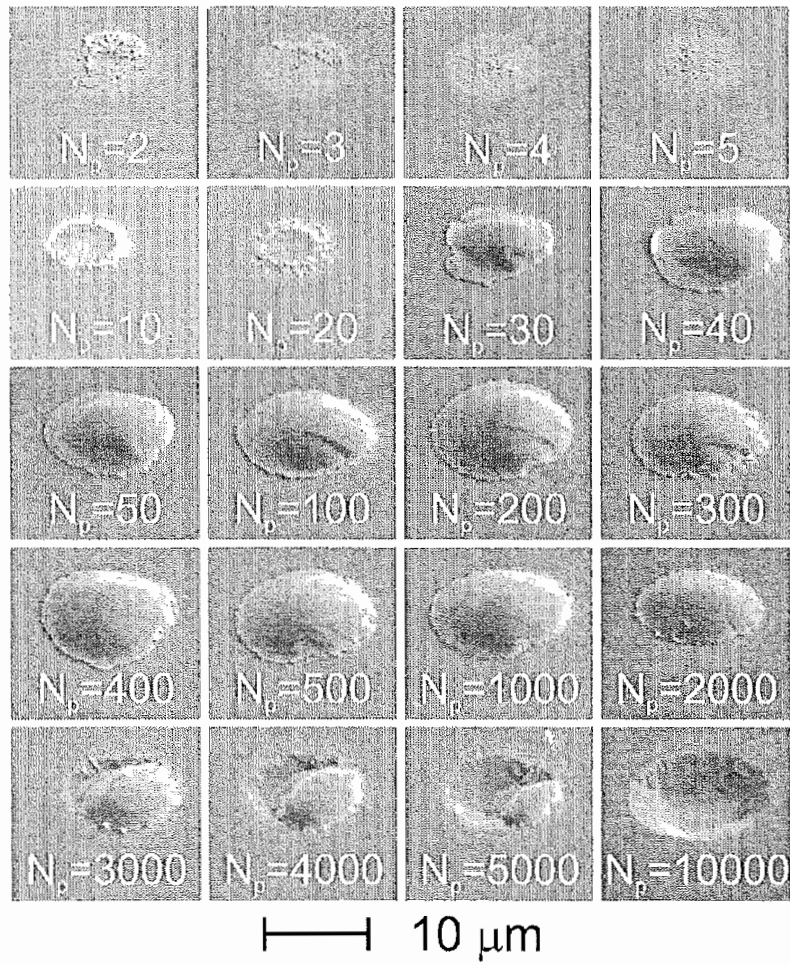


Figure 3: SEM micrographs of deposits of fused silica produced by varying  $N_p$ , with fluence  $0.4 \text{ J/cm}^2$ .

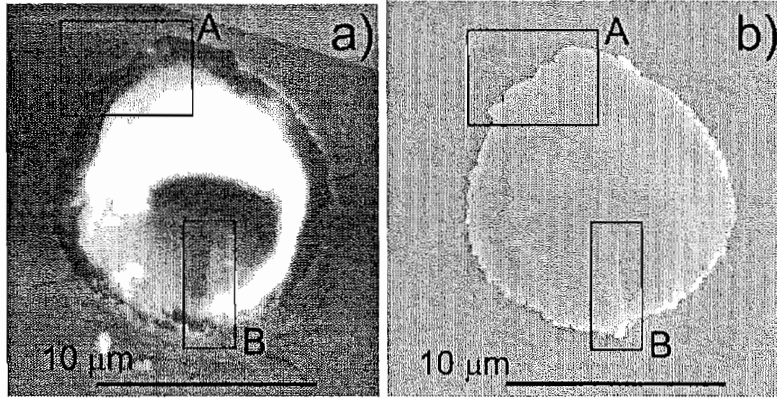


Figure 4: SEM micrographs of a hole in fused silica (a) and corresponding silica deposit on Si (b).  $N_p = 500$ , fluence  $0.4 \text{ J/cm}^2$ .



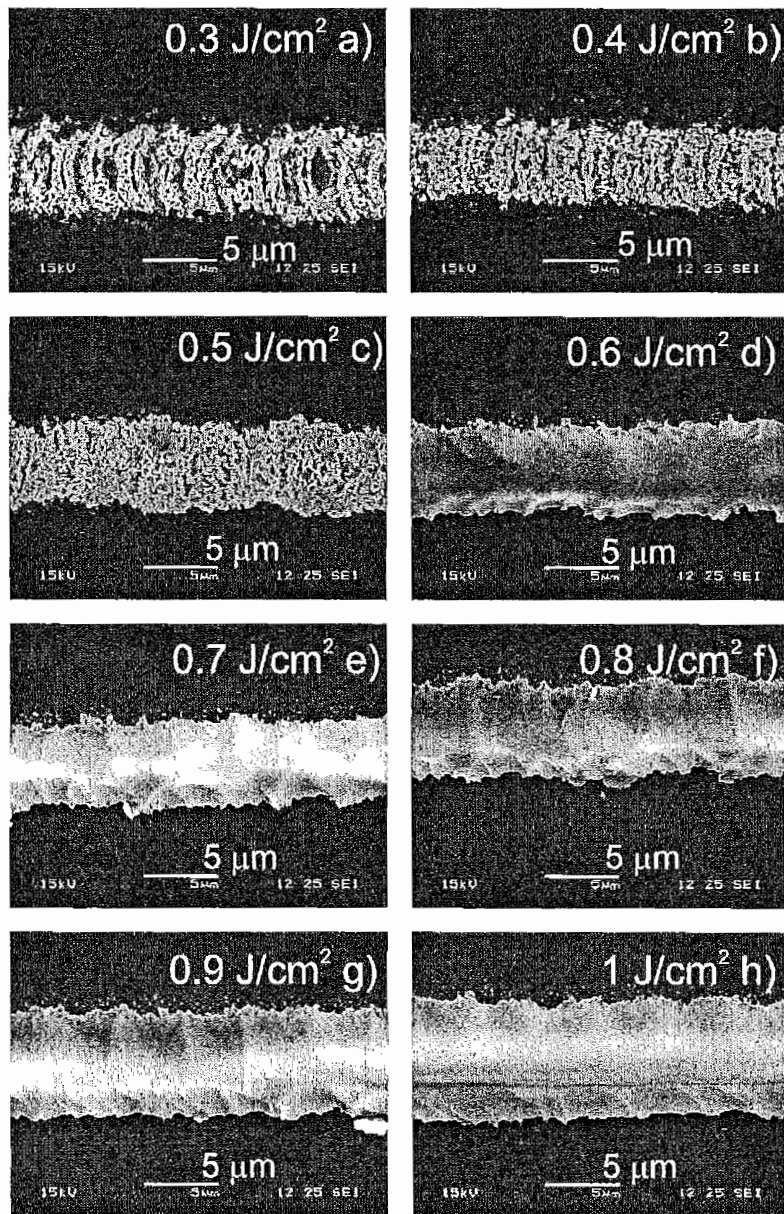


Figure 5: SEM micrographs of line structures obtained by raster-scanning laser at  $v = 1.1$  mm/s with indicated fluence.

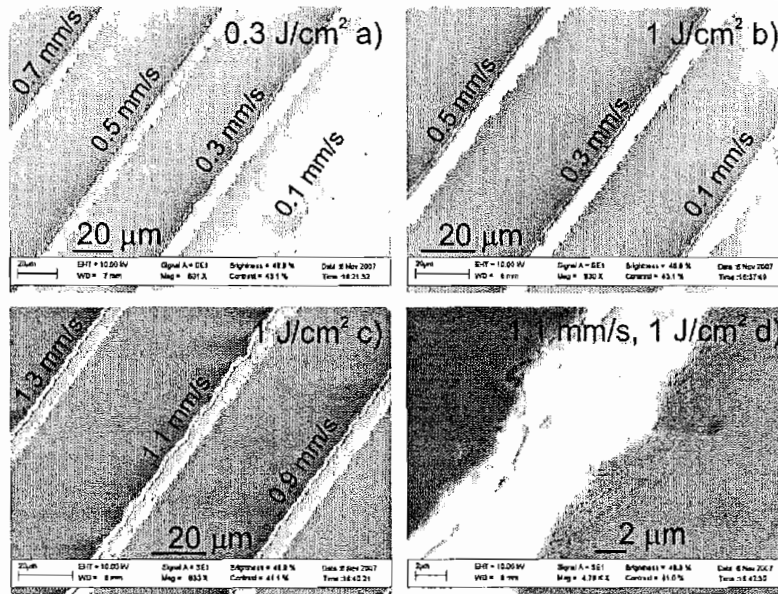


Figure 6: SEM micrographs of channels in fused silica substrate after exposure to 0.3 (a) and 1 J/cm<sup>2</sup> (b,c) with indicated raster speeds. Close up of channel with 1 J/cm<sup>2</sup> written at 1.1 mm/s (d).

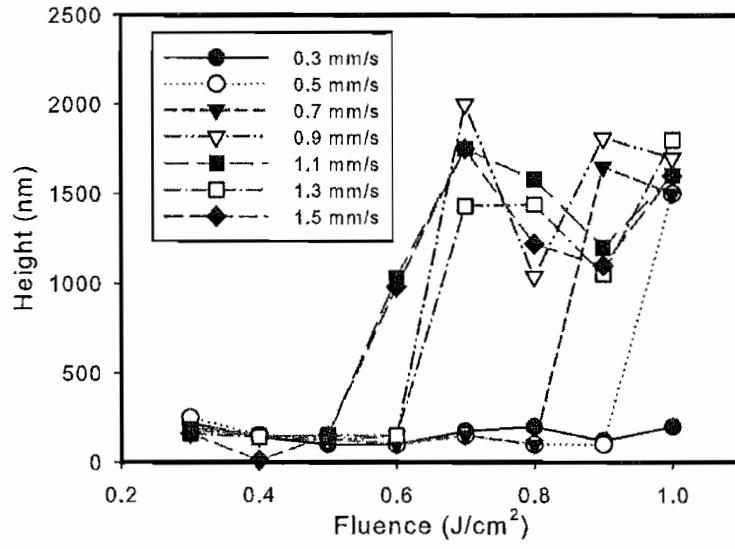


Figure 7: Plot of maximum height of silica lines as a function of fluence and raster speed.

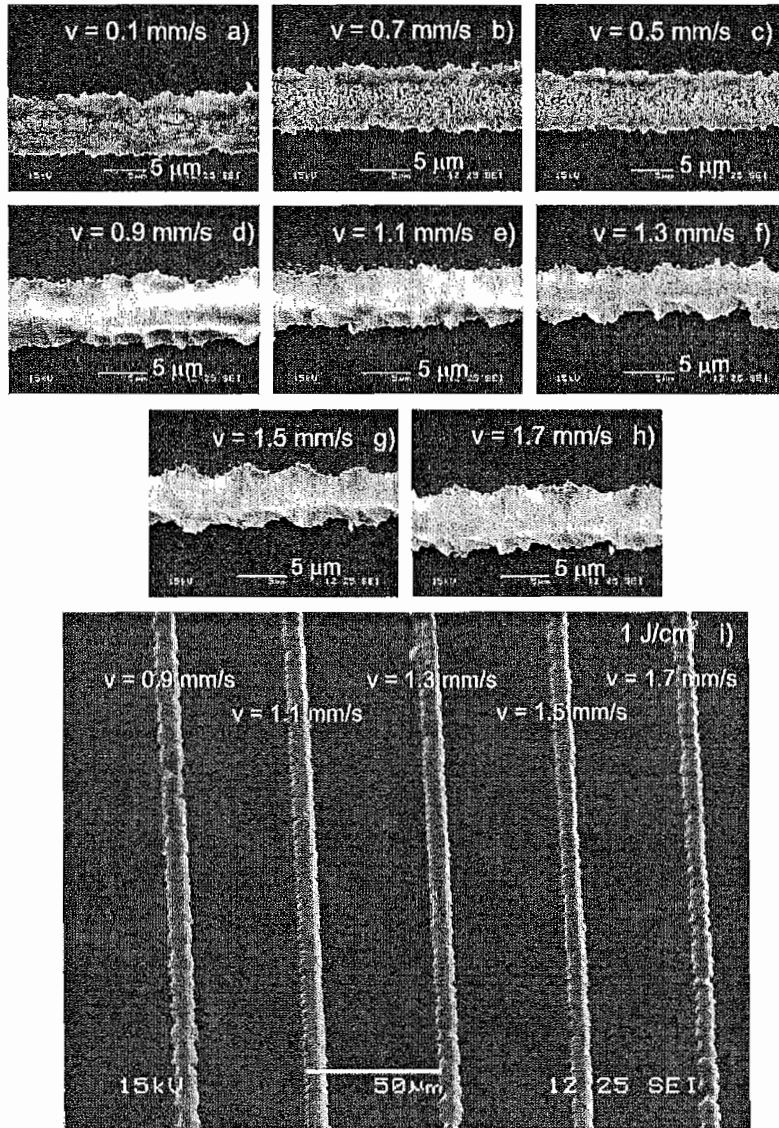


Figure 8: SEM micrographs of line structures obtained by varying raster speed  $v$  with fluence  $0.7 \text{ J/cm}^2$  (a-h) and zoomed-out view of silica lines with  $1 \text{ J/cm}^2$  (i).